Neuromodulation: Technology at the Neural Interface

Received: November 29, 2022 Revised: February 27, 2023 Accepted: March 6, 2023

https://doi.org/10.1016/j.neurom.2023.03.002

Cardiovascular Response to Intraneural Right Vagus Nerve Stimulation in Adult Minipig

Filippo Agnesi, PhD[1,a]; Ciro Zinno, MSc[1,a]; Ivo Strauss, PhD[2]; Anar Dushpanova, MD, PhD[3,4]; Valentina Casieri, MD, PhD[3,5]; Fabio Bernini, BSc[5]; Domiziana Terlizzi, VMD[6]; Khatia Gabisonia, MD, PhD[5]; Vincenzo Lionetti, MD, PhD[3,5]; Silvestro Micera, PhD[1,7]

ABSTRACT

Objective: This study explored intraneural stimulation of the right thoracic vagus nerve (VN) in sexually mature male minipigs to modulate safe heart rate and blood pressure response.

Material and Methods: We employed an intraneural electrode designed for the VN of pigs to perform VN stimulation (VNS). This was delivered using different numbers of contacts on the electrode and different stimulation parameters (amplitude, frequency, and pulse width), identifying the most suitable stimulation configuration. All the parameter ranges had been selected from a computational cardiovascular system model.

Results: Clinically relevant responses were observed when stimulating with low current intensities and relatively low frequencies delivered with a single contact. Selecting a biphasic, charge-balanced square wave for VNS with a current amplitude of 500 μA, frequency of 10 Hz, and pulse width of 200 μs, we obtained heart rate reduction of 7.67 ± 5.19 beats per minute, systolic pressure reduction of 5.75 ± 2.59 mmHg, and diastolic pressure reduction of 3.39 ± 1.44 mmHg.

Conclusion: Heart rate modulation was obtained without inducing any observable adverse effects, underlining the high selectivity of the intraneural approach.

Keywords: Bioelectronic medicine, heart rate modulation, intraneural electrode, intraneural stimulation, vagus nerve stimulation

Conflict of Interest: The authors reported no conflict of interest.

INTRODUCTION

The vagus nerve (VN) is the main effector of the parasympathetic nervous system, which is divided into two branches (right VN and left VN), targeting a variety of structures including the tongue, pharynx, bronchi, lungs, heart, esophagus, stomach, colon, liver, duodenum, and pancreas.[1] Owing to its multifascicled internal structure, it is responsible for a wide variety of regulatory functions including respiratory, cardiac, and gastric functions; immune homeostasis; and proinflammatory responses via the inflammatory reflex.[2,3] The VN is a cranial nerve composed of both afferent and efferent fibers, with a vast majority being afferent (up to 90%) than efferent (10%).[4] Afferent fibers carry information from the body up to the central nuclei; thus they can be interfaced to record and monitor the physiological status of many peripheral organs and networks innervated by the VN. In addition, by modulating the

Address correspondence to: Silvestro Micera, PhD, BioRobotics Institute, Department of Excellence in Robotics & AI, Scuola Superiore Sant'Anna, Viale Rinaldo Piaggio 34, Pontedera 56025, Pisa, Italy. Email: silvestro.micera@santannapisa.it

[1] BioRobotics Institute, Department of Excellence in Robotics & AI, Scuola Superiore Sant'Anna, Pisa, Italy;
[2] Institut für Mikrosystemtechnik, University of Frieberg, IMTEK, Freiburg, Germany;
[3] Unit of Translational Critical Care Medicine, Laboratory of Basic and Applied Medical Sciences, Interdisciplinary Research Center "Health Science," Scuola Superiore Sant'Anna, Pisa, Italy;
[4] Health Research Institute, Al-Farabi Kazakh National University, Almaty, Kazakhstan;
[5] BioMedLab, Scuola Superiore Sant'Anna, Pisa, Italy;
[6] Fondazione Toscana G. Monasterio, Pisa, Italy; and
[7] Bertarelli Foundation Chair in Translational NeuroEngineering, Centre for Neuroprosthetics and Institute of Bioengineering, École Polytechnique Fédérale de Lausanne, Lausanne, Switzerland

[a]Indicates equal contribution.

For more information on author guidelines, an explanation of our peer review process, and conflict of interest informed consent policies, please see the journal's Guide for Authors.

Source(s) of financial support: The European Commission through the H2020-FETPROACT-2018-2020 NEUHEART Project #824071 funded this study.

activity of efferent fibers it is possible to influence the behavior of the target organs by using physical stimuli, such as electrical current. Vagus nerve stimulation (VNS) consists of the activation of the VN fibers to modulate several physiological functions.[5] VNS is a US Food and Drug Administration–approved technique for drug-resistant epilepsy, depression, and cluster headaches. Several studies have been carried out in the last decade to investigate the role of VNS in the treatment of metabolic and cardiovascular disorders, in particular, obesity and diabetes type 2,[5–7] inflammatory conditions (eg, rheumatoid arthritis),[8–10] and hypertension.[11,12]

Among all the different indications, the cardiovascular ones are of particular interest because they are the leading cause of morbidity and mortality, accounting for 17 million deaths in 2013.[13] VNS can be exploited to treat cardiac disease because the VN richly innervates the heart, and its stimulation produces different effects according to the specific innervated region.[14] In the last decade, indeed, VNS has been shown to be beneficial for treating heart failure (HF). Moreover, implantable VNS using a cuff electrode placed on the right VN can improve heart rate variability (HRV)[11] in acute settings, whereas HRV and blood pressure (BP) levels return to baseline by turning the VNS off. In this scenario, VNS optimized autonomic regulation by significantly increasing HRV during transient stimulation may improve cardiac function in the long term. This perspective is clinically relevant.

In hospital setting, beta blockers provide inhibition of sympathetic overexcitation; however, there are few therapies aimed at increasing vagal activity.[15] For example, several groups applied VNS to normalize parasympathetic activity in HF patients.[16–18] Because the literature seems to suggest that the right VN has a stronger influence on the sino-atrial node and provides cardioinhibitory tone,[19] we selected the right VN as the VNS target in our study. Gold et al[16] applied open-loop and heartbeat-synchronized stimulation to the cervical region of the right VN using a cuff electrode in patients with HF.[16] A similar study was led for the NEural Cardiac TherApy foR Heart Failure (NECTAR-HF) trial.[20] Although the treatment was well tolerated by patients and slightly improved hemodynamic parameters, VNS did not improve the outcome of patients with HF at 18 months because of insufficient stimulation energy. Another approach was pursued for the Autonomic Neural Regulation Therapy to Enhance Myocardial Function in Heart Failure (ANTHEM-HF) trial,[17,21] in which an open-loop chronic continuous stimulation was performed (cyclic stimulation 14 seconds on and 66 seconds off, 10 Hz, 130 μs pulse width [PW], left/right VN implant). Comparing the results of the ANTHEM-HF trial with the INcrease Of VAgal TonE in CHF (INOVATE-HF) trial,[21] the ANTHEM-HF trial showed improved results in terms of heart rate (HR), HRV, and hemodynamic parameters; however, some of these improvements were lost in a long-term follow-up study.[22]

Therefore, new strategies for precise vagus neuromodulation are desirable. One of the main limitations of VNS is currently the lack of selectivity in stimulation. The autonomic nervous system, and in particular, the VN, is responsible for a variety of physiological functions, each modulated by a different group of fascicles. The fascicle cluster according to the function they accomplish in different regions of the VN along its longitudinal axis.[2] Being able to selectively activate only the fascicle of interest is crucial to increase the effectiveness of VNS-based therapies. Cardiac-related fascicles are among the smallest in the VN.[2,23] Their activation using extraneural cuff electrodes requires a high amount of current to be delivered, which could cause adverse effects because of the stimulation (ie, cough, neck muscle contraction, dyspnea[24]). A possible solution to overcome this limitation is the use of devices capable of selectively interface the internal fascicles of the VN. To this end, we tested multichannel intraneural electrodes. It is conceivable that this approach could improve the effectiveness of cardiac stimulation by selectively activating the vagal fibers of interest without inducing adverse effects.[25]

To the best of our knowledge, there are no studies on the modulation of the cardiovascular response to right VNS using intraneural electrodes. In this study, we assessed the cardiovascular effect of intraneural right VNS in adult minipigs, which is the animal model most resembling the diameter and fascicular complexity of the human cervical VN.[26]

MATERIALS AND METHODS

Electrode Design Fabrication

The intraneural electrode is a thin-film polyimide device, similar to the Transversal Intrafascicular Multichannel Electrode (TIME) concept.[27] It has 16 channels with active sites (circular contacts, 80 μm diameter) made of gold and coated with iridium oxide for better electrochemical properties. The fabrication process has been described in detail elsewhere.[27–29] In brief, a first layer of Ti/Al (20/100 nm) was deposited on a silicon wafer through e-beam evaporation. A 5-μm thick layer of polyimide (PI2611, HD Microsystems GmbH, Neu-Isenburg, Germany) was then poured through spin coating, followed by a thermal curing process. The first photolithographic step consisted of spin coating, baking, exposing, and developing a 4-μm thick photoresist (ECI 3027). Then, a conductive layer of Ti/Pt/IrOx (25/300/400 nm) was sputtered (AC450, Alliance Concept, Annecy, France) and patterned thanks to lift-off. A second layer of polyimide, 5-μm thick was spin-coated and cured for tracks isolation and encapsulation. Another photolithographic step (AZ10XT 12 μm) was performed, followed by O2-based reactive ion etching (RIE). The RIE was used to obtain the desired shape of the device and expose the active sites and the connecting pads of the electrode. The devices were then released through anodic dissolution of aluminum in a 1.5 V bias in saturated sodium chloride solution. We designed the dimension of the electrode and its active site distribution according to the internal structure of the VN based on histological studies.[29]

The electrode was connected to a custom flexible PCB (Printed Circuit Board, Phoenix, Italy) using silver glue to ease its handling and the implantation procedure. Biocompatible UV glue (Dymax M-UR, Germany) was poured to cover the pads of the PCB, to avoid contact between the silver glue and the biological tissue. Following the concept of the TIME, the electrode was folded and a suture thread with a loop on one side and a needle on the other side was inserted to perform the implantation.

Surgical Preparation

The protocol for all animal studies (no. 76/2014 PR) was approved by the Italian Ministry of Health and was in accordance with the Italian law (D.lgs. 26/2014). Five healthy adult male Göttingen minipigs (Ellegaard Göttingen Minipigs A/S, Dalmose, Denmark; avg body weight 35 kg) were included in this study. Animals were premedicated using Zoletil® (10 mg/kg) and Stressnil (1 mg/kg). Each animal was anesthetized using propofol (2 mg/kg intravenously) and maintained under 1% to 2% sevoflurane in air enriched by 50% oxygen during mechanical ventilation.[30,31] Throughout the experiments, the animals received an infusion of 500 mL of sodium chloride (0.9%) solution to prevent dehydration.

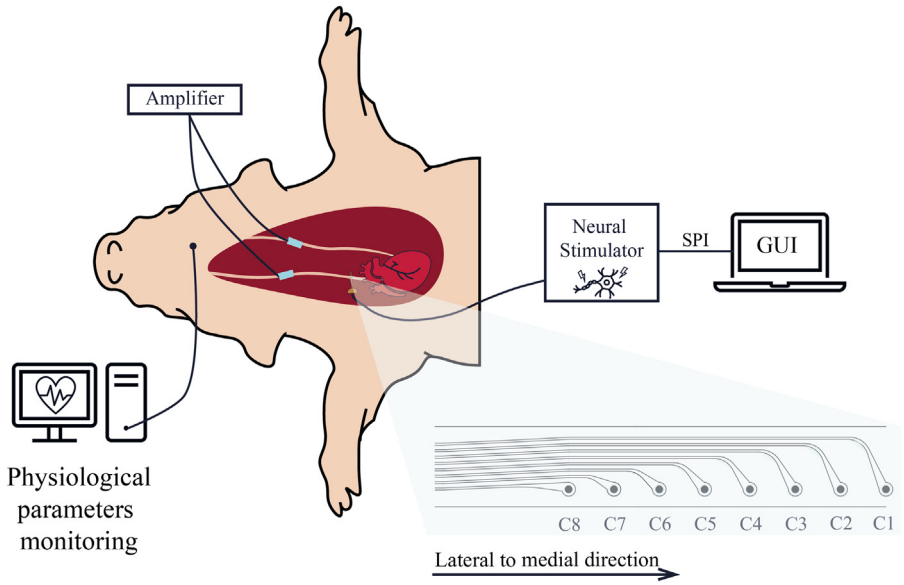

Figure 1. Representation of the implant. The intraneural electrode is inserted in the right thoracic VN, in proximity to the heart, in a lateral to medial direction. The current is delivered through a custom neural stimulator controlled by a graphic user interface.[32] The cuff electrodes are implanted between the cervical and thoracic region of both left and right VN. SPI, serial peripheral interface. [Color figure can be viewed at www.neuromodulationjournal.org]

We performed a longitudinal incision followed by a sternotomy. We used blunt dissection to expose the VN both at the cervical and thoracic level. We implanted four channel recording cuffs (WPI, Sarasota, FL) around the right VN at the cervical level. We inserted the intraneural electrode transversally in the right VN at the thoracic level close to the heart (Fig. 1) and connected to a custom neural stimulator.[32] The distance between the intraneural electrode and the cuff electrode was between 5 and 8 mm depending on the anatomy of each animal.

Data Collection and Analysis

We performed recordings with 10 seconds of baseline followed by 1 minute of stimulation and a poststimulation period of 1 minute.

Differential recordings of the VN activity were obtained from the implanted cuff using a TDT system (Tucker Davis Technologies, Alachua, FL) at 24k samples per second. We performed data processing and analysis using custom Matlab (Mathworks, Natick, MA) software. The electroneurography data were filtered using a 4th-order Butterworth 50 Hz lowpass filter. The timing of each stimulation pulse was identified using the stimulation artifacts. Stimulation-triggered averaging was used to evaluate the presence of evoked compound action potentials (ECAPS).

We measured arterial BP from the femoral artery and recorded at 1.5k samples per second. We recorded systolic and diastolic arterial BP for each heartbeat and filtered to remove the variation induced by the breathing cycle. We performed continuous electrocardiogram monitoring to measure HR and to evaluate cardiac rhythm. We also evaluated electromechanical coupling activity at each cardiac cycle. Instantaneous HR was also simultaneously derived from the arterial BP signal inverting the time interval between each subsequent systolic BP peak. BP and HR were baseline normalized by subtracting the average of the prestimulation period. The reduction in BP and HR induced by the stimulation was calculated as the difference between the average of the prestimulation period and the minimum value during the stimulation period.

VNS Parameters

We performed VNS using cathodic first, charge-balanced, square waves with intensities between 100 and 500 μA, frequency between 1 and 30 Hz, and PW between 50 and 200 μs. The ranges were selected starting from a model developed in literature.[33] To identify the electrode's active site yielding the best physiological response, we initially performed stimulation (500 μA, 30 Hz, 200 ms PW) performed using all the contacts on one side of the electrode (eight contacts active simultaneously) and then with all the contacts on the opposite side. We selected the side yielding the largest response and tested all its eight contacts one at a time. Then, we selected and used the contact producing the larger response to test different stimulation intensities (100, 200, 300, 400, and 500 μA; 30 Hz; 200 ms PW), different frequencies (1, 2, 3, 5, 10, 15, 20, 25, and 30 Hz; 500 μA; 200 ms PW) and different PW (50, 100, 150, and 200 ms; 500 μA; 30 Hz). Owing to time constraints during the experiments, not all parameter sweeps (intensity, frequency, and PW) were performed on each animal. Intensity and PW sweeps were performed on $n = 3$ animals, whereas frequency sweeps were performed on $n = 4$ animals.

RESULTS

When stimulating through activating all the eight contacts on each side of the electrode, we were able to observe physiological responses for both sides of the electrode in three out of the five animals with one side of the electrode producing a stronger response in all three animals. In the remaining two animals, we observed physiological responses only for one side of the electrode.

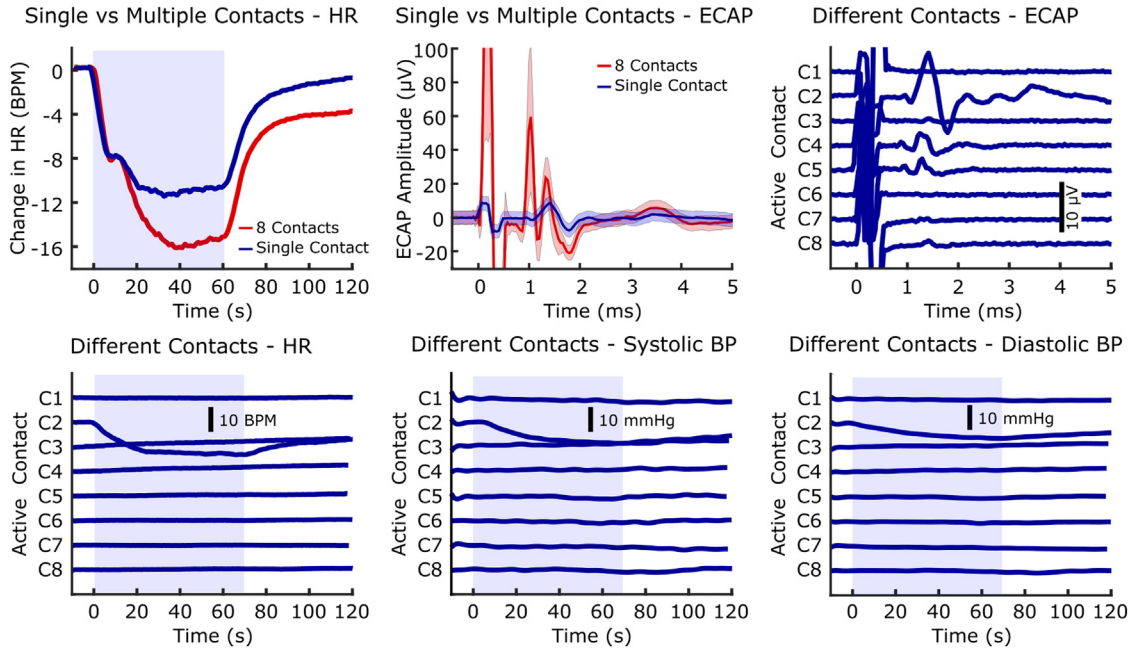

Figure 2. Physiological response to stimulation with different contacts. Top left: example of a response to eight-contact and single-contact stimulation (500 μA/contact). Despite an eight-fold increase in stimulation current, only a moderate increase in the physiological response is seen. Top middle: examples of ECAP response to eight-contact and single-contact stimulation. The magnitude and the shape of the ECAP response to an eight-contact stimulation suggest an activation of a broader spectrum of VN fibers. Top right: ECAP recording with varying stimulation contact. Bottom: HR (left), systolic BP (middle), and diastolic BP (right) responses with varying stimulation contact. Cardiac modulation is seen only with the C2 contact, whereas ECAPs are present on other channels, suggesting a high degree of selectivity for intraneural stimulation. [Color figure can be viewed at www.neuromodulationjournal.org]

It was always possible to elicit physiological responses by delivering stimulation using a single active contact except for one animal, in which activating two neighboring contacts was necessary. When activating single contacts, in three animals, only one of the contacts was able to elicit physiological responses (ie, no responses were observed when activating the other seven contacts), whereas in one

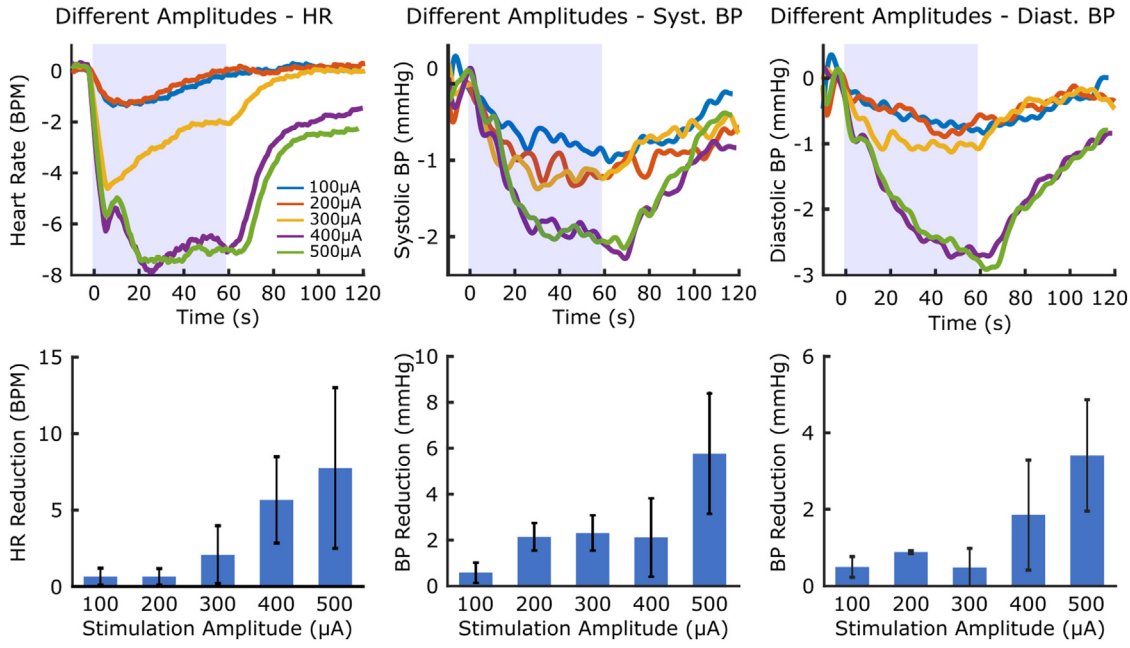

Figure 3. Physiological responses to different stimulation amplitudes. Top: HR (left), systolic BP (middle), and diastolic BP (right) responses to different stimulation amplitudes. Higher responses can be observed when 400 to 500 μA amplitude current was delivered, suggesting a threshold effect of fiber activation. Bottom: HR (left), systolic BP (middle), and diastolic BP (right) reductions across different animals (n = 3). The magnitude of the response was different when the stimulation amplitude was varied, with the highest changes observed after the threshold was reached. Diast., diastolic; Syst., systolic. [Color figure can be viewed at www.neuromodulationjournal.org]

Table 1. Reduction in Monitored Physiological Parameters During VNS With Varying Amplitude.

Physiological variation	100 μA	200 μA	300 μA	400 μA	500 μA
ΔHR (BPM)	0.63 ± 0.55	0.63 ± 0.53	2.05 ± 1.87	5.57 ± 2.79	7.67 ± 5.19
ΔSyst. BP (mmHg)	0.62 ± 0.43	2.17 ± 0.6	2.33 ± 0.76	2.14 ± 1.68	5.75 ± 2.59
ΔDiast. BP (mmHg)	0.51 ± 0.27	0.89 ± 0.04	0.49 ± 0.5	1.85 ± 1.43	3.39 ± 1.44

Diast, diastolic; Syst, systolic.

animal, we observed responses from four contacts (activated one at a time). In the last animal, the response was visible only when activating two neighboring contacts simultaneously.

As can be seen in Figure 2 (top left), stimulation delivered by activating all eight contacts produced a larger physiological response than that delivered by activating a single contact. Nevertheless, the responses were generally comparable in magnitude even if the current applied was one-eighth in the case of the single contact. In contrast, ECAPS generated by activating eight contacts were significantly larger than those that were generated by activating a single contact as can be seen in Figure 2 (top center). Moreover, also the shape of the ECAP was different, suggesting the recruitment of additional fibers during stimulation performed by activating eight contacts.

Figure 2 (top right and bottom row) shows representative ECAPS, HR, systolic and diastolic BP observed during the stimulation performed with each of the eight contacts on one side of the electrode. Although it is possible to see ECAPS generated activating different contacts, we observed cardiac responses only during the activation of one contact. Figure 3 shows the effect of varying VNS intensity on the cardiac response.

Figure 3 (top row) shows representative HR, systolic BP, and diastolic BP responses to VNS of varying intensities. We performed VNS by activating the same contact with varying intensities in $n = 3$ animals. The reduction of HR, systolic BP, and diastolic BP are summarized in Table 1. In Figure 3 (top row), it is possible to appreciate a threshold effect in the responses. When stimulating with amplitudes of up to 300 μA, minimal responses were observed and increasing the stimulation to up to 400 to 500 μA, a marked response could be observed. A similar behavior is reflected in the slope of the decay, with steeper reduction obtained with increasing amplitude.

Figure 4 (top row) shows the effect of varying VNS frequency on cardiac response. Figure 4 (top row) shows representative HR, systolic BP, and diastolic BP responses to VNS delivered using different frequencies. We performed VNS by activating the same contact using varying frequencies in $n = 4$ animals. The reduction of HR, systolic BP, and diastolic BP are summarized in Table 2. Like intensity, in Figure 4 (top row), it is possible to highlight a threshold effect in frequency, with a threshold set to 5 Hz.

Figure 5 (top row) shows the effect of varying VNS PW on cardiac response. Figure 5 shows representative HR (top left), systolic BP

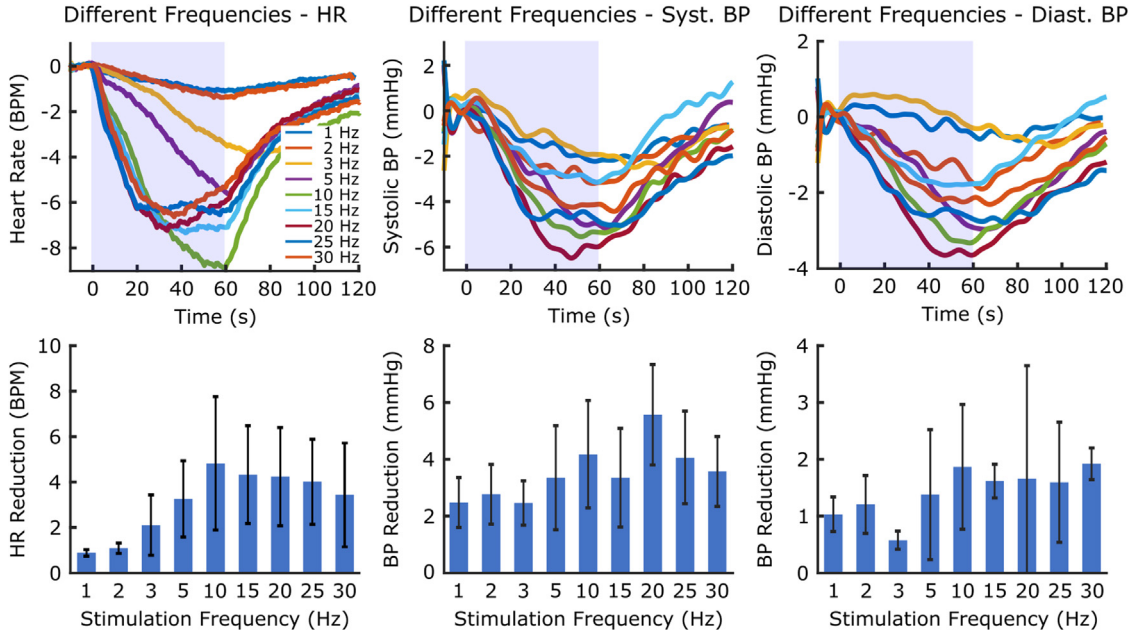

Figure 4. Physiological responses to different stimulation frequencies. Top: HR (left), systolic BP (middle), and diastolic BP (right) responses to different stimulation frequencies. The dynamic of the response was different when the stimulation frequency was varied, with a more rapid decrease obtained with higher frequency. The plateau for the decrease of the physiological signals was achieved at 10 (HR) and 20 (systolic and diastolic BP) Hz frequencies. Bottom: HR (left), systolic BP (middle), diastolic BP (right) reductions across different animals ($n = 4$). The physiological response increased as frequency increased up to a maximum, after which it plateaued. Diast., diastolic; Syst., systolic. [Color figure can be viewed at www.neuromodulationjournal.org]

Table 2. Reduction in Monitored Physiological Parameters During VNS With Varying Frequency.

Physiological variation	1 Hz	2 Hz	3 Hz	5 Hz	10 Hz	15 Hz	20 Hz	25 Hz	30 Hz
ΔHR (BPM)	0.9 ± 0.15	1.11 ± 0.22	2.11 ± 1.31	3.25 ± 1.66	4.8 ± 2.89	4.13 ± 2.13	4.22 ± 2.14	4 ± 1.85	3.43 ± 2.27
ΔSyst. BP (mmHg)	2.48 ± 0.88	2.76 ± 1.05	2.46 ± 0.77	3.35 ± 1.82	4.17 ± 1.87	3.34 ± 1.72	5.54 ± 1.76	4.05 ± 1.61	3.57 ± 1.23
ΔDiast. BP (mmHg)	1.03 ± 0.3	1.21 ± 0.5	0.58 ± 0.16	1.38 ± 1.13	1.86 ± 1.08	1.61 ± 0.29	1.66 ± 1.97	1.59 ± 1.05	1.91 ± 0.28

Diast, diastolic; Syst, systolic.

(top middle), and diastolic BP (top right) responses to VNS delivered using PW. We performed VNS by activating the same contact using varying PW in $n = 3$ animals. The reduction of HR, systolic BP, and diastolic BP are summarized in Table 3.

During all the stimulation sessions, we did not observe any arrythmia or alteration from the sinus rhythm. Moreover, there was no evidence of visible adverse effects (ie, neck contractions, cough).

DISCUSSION

The results of this study show that unilateral right VNS delivered using intraneural electrodes modulate HR without inducing arrhythmia and provide preliminary information on the most efficient stimulation parameters for this application. The chronotropic cardiac responses elicited during stimulation were characterized by a rapid decrease of HR immediately after initiation of the stimulation, generally reaching a plateau after about 20 seconds. HR remained lowered during the stimulation and started returning to baseline as soon as stimulation was discontinued. Systolic and diastolic pressures similarly decreased during intraneural stimulation of the right VN, although the onset of BP decay was delayed compared with that of HR. Indeed, the peak reduction of systolic BP in response to HR variation reached its maximum after about 40 seconds of stimulation, while it is delayed by approximately 2 to 4 seconds compared with the resting HR.[34] Likewise, when the stimulation is discontinued, a similar delayed response can be seen. The HR immediately increases and starts to return to baseline conditions, while the BP is delayed. Moreover, the time necessary for HR to return to baseline seems to be shorter than that for BP. The time delay difference in dynamics seems to suggest that the observed BP reduction is likely secondary to the HR decrease because of our pattern of right VNS. Although both reductions in HR and BP are clinically relevant, the magnitude of the rhythmic reduction in HR from baseline values is more significant than that in BP. Our data are in accord with previous experimental findings demonstrating that the autonomic modulation of HR is an even less important determinant of BP powers. Indeed, the regulation of BP powers are mainly under sympathetic cardiovascular influences.[34]

Intraneural electrode represents a more invasive solution than the cuff electrodes commonly used but can afford a higher level of selectivity because of the small size of the active contacts and their proximity to nerve fascicles.

Large active stimulation surfaces and higher intensities of current delivered will generate larger electric fields activating larger volumes of neuronal tissue and are therefore expected to induce

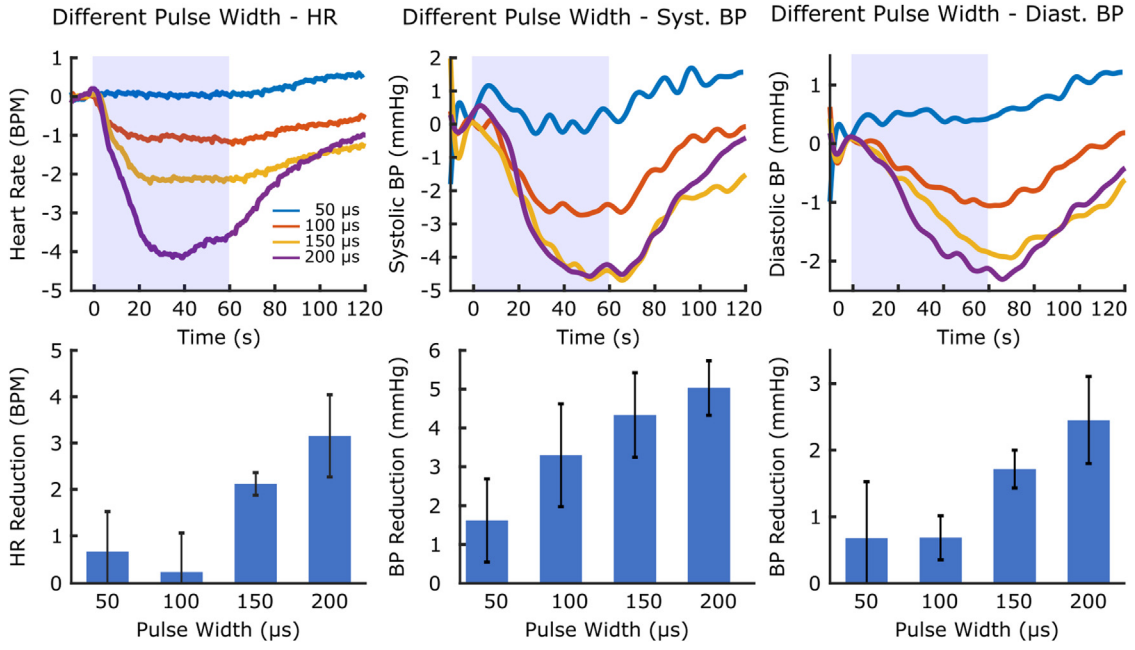

Figure 5. Physiological responses to different stimulation PWs. Top: HR (left), systolic BP (middle), and diastolic BP (right) responses to different stimulation PWs. Bottom: HR (left), systolic BP (middle), and diastolic BP (right) reductions across different animals ($n = 3$). A PW of > 150 µs was necessary to obtain a noticeable physiological response, suggesting that the fibers mediating the response have a small diameter. Diast., diastolic; Syst., systolic. [Color figure can be viewed at www.neuromodulationjournal.org]

Table 3. Reduction in Monitored Physiological Parameters During VNS With Varying Pulse Width.

Physiological variation	50 μs	100 μs	150 μs	200 μs
ΔHR (BPM)	0.69 ± 0.84	0.24 ± 0.83	2.12 ± 0.24	3.14 ± 0.88
ΔSyst. BP (mmHg)	1.61 ± 1.06	3.29 ± 1.31	4.03 ± 1.08	5 ± 0.7
ΔDiast. BP (mmHg)	0.68 ± 0.84	0.68 ± 0.33	1.7 ± 0.28	2.43 ± 0.65

Diast, diastolic; Syst, systolic.

larger physiological responses. Indeed, the administration of current (500 μA) to each of the eight contacts on one side of the intraneural electrode led to a larger HR decrease than the delivery of similar current to a single active contact (Fig. 2, top left). Despite this, the two evoked responses were of similar magnitude, suggesting progressive activation of a small number of cardiac VN fibers during intraneural stimulation with all eight contacts is satisfactory. We cannot rule out the possibility that, once all cardiac fibers have been captured, further increases in the electrical field of stimulation do not help increase the effectiveness and represent unnecessary energy consumption for the batteries of an implanted stimulator. In addition, it is plausible that larger fields produced by multicontact stimulation can produce cross-talk, activating multiple VN fascicles responsible for different functions. Indeed Figure 2 (top center) supports this hypothesis. Despite a similar magnitude of HR reductions, ECAPS recorded during stimulation delivered using eight contacts are not only quite large (the beta potential recorded between 1 and 2 ms is more than twice when stimulation is delivered using eight contacts) but also suggest the recruitment of different fiber types (the alpha potential recorded around 1 ms and the gamma potential recorded between 3 and 4 ms are present only when stimulation is delivered using eight contacts). Intraneural stimulation showed a high degree of selectivity when performed by activating each of the eight contacts one at a time. Although Figure 2 (top right) shows ECAPS being evoked by stimulation delivered on contacts C2, 4, 5, 7, and 8, we observed cardiac responses only during stimulation with contact C2. In addition, except for a single animal, we observed physiological responses only during the activation of one of the eight contacts (or two neighboring contacts in one animal) but not for the remaining contacts. We can suppose that small electric fields, localized close to the target VN fibers, are required for selective activation of cardiac efferent responsible for chronotropic modulation of heart activity, without affecting the fascicles responsible for respiration, cough reflex, and neck contractions.

In this regard, our approach can slow down the HR (reduction by 8–15 beats per minute [BPM]) in anesthetized and mechanically ventilated healthy minipigs without eliciting any detectable acute adverse effects, such as neck muscle contractions. To the best of our knowledge, this is the first study exploring right VNS with intraneural electrodes for HR modulation. Buschman et al[35] used helical electrodes around the right cervical VN to modulate the HR in anesthetized pigs. Using a biphasic square wave (100 Hz, 5 mA, 200 μs PW), they obtained an increase in the R-R interval of up to 40% compared with baseline condition (120 BPM). So far, multichannel cuff electrodes are employed to obtain selective VN stimulation.[12,36,37] Blanz et al[37] employed a cuff electrode with six contacts distributed along the longitudinal and radial axis of the nerve to perform VNS in pigs, targeting the right cervical VN. The results in terms of VNS efficacy are impressive, with an HR reduction of up to 30 to 40 BPM. However, the current delivered through the electrode contacts was significantly higher (up to 5 mA), because of an extraneural approach, and the stimulation site was different (cervical vs thoracic). Owing to the higher threshold of the cardiac fibers, stimulating using cuff electrodes, it was not possible to elicit a cardiac response without undesired muscle activation of the neck. Indeed, it is conceivable that our results were affected by the anesthesia protocol. Blanz et al[37] administered isoflurane, whereas in our experimental sessions, animals were anesthetized using sevoflurane. It has been shown in human[38] and animal[39] studies that isoflurane administration results in higher HR than sevoflurane even during controlled ventilation.[40] Although sevoflurane is known to partly dampen sympathetic baroreflex sensitivity in response to reduced systemic vascular resistances, the baroreceptor response remains mainly intact with isoflurane, and cardiac output in the presence of lower afterload remains stable because of increased HR.[41] In fact, the magnitude of HR reduction during VNS is most appreciable at higher basal HR values. A similar approach has been pursued by Plachta et al[12,36] for the treatment of hypertension in rats. By stimulating the left cervical VN with multichannel cuff electrodes (eight arrays of tripoles), it was possible to obtain a reduction in BP and HR with similar stimulation parameters. Moreover, this effect was amplified using a stimulation paradigm consisting of cardiac-synchronized stimulation,[12] improving at the same time energy efficiency.

To optimize stimulation parameters, we performed a stimulation ramp in which we systematically varied intensity, frequency, and PW one at a time. The sets of parameters explored were selected based on a model describing the effect of VNS on the cardiac system.[33] As shown in Figure 3, response to current injection proportionally increased with stimulation amplitude. As expected, lower amplitudes failed to elicit significant physiological responses; once the amplitude reached a personalized threshold level (about 300 or 400 μA) the physiological response becomes clearly detectable. Notably, no increase in physiological responses between 400 and 500 μA was observed in two of the three animals. It is likely possible that in the third animal, the electrode position was suboptimal, further away from the cardiac fascicles than in the other two animals. Therefore, even injecting the highest current amplitude (500 μA) we probably were not able to recruit all the cardiac fascicles, thus we could not observe plateauing of the response. Together with the limited increase in response observed between stimulations performed by activating all eight contacts and only one contact, our results suggest the presence of a "sweet spot" for stimulation intensity. This is not surprising considering the geometry of the electrode and VN fascicles. The electrode is inserted transversally with its main axis roughly perpendicular to the fascicles in the VN. The selectivity shown during the activation of single contacts suggests that the cardiac fascicle needs to be in close proximity to the activated contact because shifting the stimulation field by 235 μm is enough to stop activating the fascicle. The threshold effect observed with stimulation of

increasing amplitudes likely occurs when the electric field reaches the cardiac fascicle. Likewise, once the field reaches a size whereby it can activate all the cardiac fibers, further amplitude increase will not yield stronger responses but only increase the likelihood of side effects. For this application, we foresee it as critical to carefully define this window ("sweet spot") to maximize the desired outcomes, minimize unwanted activation, and reduce power consumption. At the same time, this underscores the need for precise positioning of the electrode within the VN, because its position needs to be close (ideally within) the target fascicle.

A similar picture emerged also when stimulating with different frequencies. As shown in Figure 4, at low frequencies (1, 2 Hz) the physiological responses were minor but increased rapidly at 3 and 5 Hz to reach a maximal response around 10 Hz. Somewhat surprisingly, further increases in intensity seemed to cause a small but progressive reduction in the observed HR response. Based on our results, a stimulation frequency of 10 Hz represents the best compromise between maximizing the physiological response and minimizing the stimulation's energy. Not surprisingly, a threshold effect is visible also when stimulating using different PW as can be seen in Figure 5. Very short PW (50 μs) were not able to elicit any physiological responses, whereas longer PW (150–200 μs) appeared to begin maxing out the elicited response. Although the number of fascicles in the thoracic VN is higher than cervical VN,[2] cardiac VN fibers have a small diameter and long PW will be therefore necessary to optimize their activation.

Another limitation of the present study consists of the use of anesthetized and mechanically ventilated animals in which the neuronal and physiological responses may be dampened. Moreover, it is possible that some fatigue could have been induced in the VN caused by repeated stimulation. This should be further investigated in future experiments by repeating the same stimulation protocols in different time scales.

Our study may open a new avenue in the modulation of other autonomic functions using the same approach for different clinical conditions (ie, arterial hypertension, inflammatory and metabolic disorders). Stimulation-induced side effects (neck muscle activation, dyspnea, coughing reflex) limit the therapeutic outcomes of VNS. Our study suggests that intraneural stimulation of VN can selectively activate the cardiac fascicles without causing overt adverse effects. The optimized parameters set would be helpful to foster the development of full implantable devices for safe cardiac rhythm modulation in patients with chronically elevated HR. There are several advantages associated with the use of intraneural electrodes in this application. Intraneural electrodes are thin-film devices presenting high mechanical flexibility. Their flexibility could lower the foreign body reaction caused by the implant, avoiding the mechanical compression imposed by cuff electrodes. However, in this context, the mechanical stability of the implant is crucial to avoid micromovements between the nerve and electrode, which could damage the nerve. Moreover, the proximity of the active contacts and target nerve fascicles allows for eliciting physiological responses at very low current intensities. This not only affords a higher level of selectivity by reducing the possibility of current spreading to off-target fibers but also significantly reduces power consumption of a fully implantable device. Consequently, implanted stimulators would have a longer lifespan, a smaller profile, and require shorter recharge time, reducing the burden on the patients. This, together with the results shown, support the feasibility of a closed-loop approach capable of modulating HR in a chronic fashion for the treatment of HF.

CONCLUSIONS

Using an eight-contact intraneural array with circular active sites size of 80 μm diameter and spacing of 235 μm, we can selectively elicit a cardiac chronotropic response, using a monopolar single-contact stimulation. The threshold effect of response (400–500 μA) is related to the geometrical relationship between the electrode contacts and the cardiac fascicles. However, because of anatomical and implantation variability, subject-specific tuning of the stimulation amplitude will be necessary to personalize the "sweet spot." For chronic applications of VNS as therapy for cardiovascular disorders, the optimal stimulation amplitude should be adjusted according to the electrode position inside the nerve and the elicited response. The ideal response should modulate selectively the HR without causing adverse effects. To obtain a rapid decrease in HR, we found 10 Hz as the optimal frequency of stimulation. Frequencies above 10 Hz do not seem to reduce the time to reach the response plateau nor elicit a stronger response. We found that 200 μs is a suitable value for the activation of the cardiac fibers inside the VN. This is reasonable considering their small diameter (< 3 μm^2), thus a long PW is needed to activate them.

Acknowledgements

The authors would like to thank the European Commission for funding the the H2020-FETPROACT-2018-2020 NEUHEART Project #824071 which made this work possible.

Authorship Statements

Filippo Agnesi, Vincenzo Lionetti, Silvestro Micera, and Ciro Zinno designed the study. Filippo Agnesi and Ciro Zinno conducted the study, including data collection and data analysis. Ivo Strauss, Anar Dushpanova, Valentina Casieri, Khatia Gabisonia, Vincenzo Lionetti, Fabio Bernini, and Domiziana Terlizzi conducted data collection processes. Filippo Agnesi and Ciro Zinno prepared the manuscript draft, with important intellectual input from Vincenzo Lionetti and Silvestro Micera. All authors approved the final version of the manuscript.

How to Cite This Article

Agnesi F., Zinno C., Strauss I., Dushpanova A., Casieri V., Bernini F., Terlizzi D., Gabisonia K., Lionetti V., Micera S. 2023. Cardiovascular Response to Intraneural Right Vagus Nerve Stimulation in Adult Minipig. Neuromodulation 2023; ■: 1–9.

REFERENCES

1. Yuan H, Silberstein SD. Vagus nerve and vagus nerve stimulation, a comprehensive review: part I. *Headache*. 2016;56:71–78. https://doi.org/10.1111/head.12647.
2. Jayaprakash N, Toth V, Song W, et al. Organ- and function-specific anatomical organization and bioelectronic modulation of the vagus nerve. Preprint. Posted online April 29, 2022. https://doi.org/10.2139/ssrn.4097124
3. Pavlov VA, Tracey KJ. The vagus nerve and the inflammatory reflex—linking immunity and metabolism. *Nat Rev Endocrinol*. 2012;8:743–754. https://doi.org/10.1038/nrendo.2012.189.

4. Fitchett A, Mastitskaya S, Aristovich K. Selective neuromodulation of the vagus nerve. *Front Neurosci*. 2021;15:685872. https://doi.org/10.3389/fnins.2021.685872.
5. Johnson RL, Wilson CG. A review of vagus nerve stimulation as a therapeutic intervention. *J Inflamm Res*. 2018;11:203–213. https://doi.org/10.2147/JIR.S163248.
6. Gouveia FV, Silk E, Davidson B, et al. A systematic review on neuromodulation therapies for reducing body weight in patients with obesity. *Obes Rev*. 2021;22: e13309. https://doi.org/10.1111/obr.13309.
7. Berthoud HR, Neuhuber WL. Vagal mechanisms as neuromodulatory targets for the treatment of metabolic disease. *Ann N Y Acad Sci*. 2019;1454:42–55. https://doi.org/10.1111/nyas.14182.
8. Carnevale L, Pallante F, Perrotta M, et al. Celiac vagus nerve stimulation recapitulates angiotensin II-induced splenic noradrenergic activation, driving egress of CD8 effector cells. *Cell Rep*. 2020;33:108494. https://doi.org/10.1016/j.celrep.2020.108494.
9. Bonaz B, Sinniger V, Pellissier S. Anti-inflammatory properties of the vagus nerve: potential therapeutic implications of vagus nerve stimulation. *J Physiol*. 2016;594:5781–5790. https://doi.org/10.1113/JP271539.
10. Kanashiro A, Shimizu Bassi G, de Queiróz Cunha F, Ulloa L. From neuroimunomodulation to bioelectronic treatment of rheumatoid arthritis. *Bioelectron Med (Lond)*. 2018;1:151–165. https://doi.org/10.2217/bem-2018-0001.
11. Annoni EM, Tolkacheva EG. Acute cardiovascular and hemodynamic effects of vagus nerve stimulation in conscious hypertensive rats. *Annu Int Conf IEEE Eng Med Biol Soc*. 2018;2018:3685–3688. https://doi.org/10.1109/EMBC.2018.8513025.
12. Plachta DTT, Zentner J, Aguirre D, Cota O, Stieglitz T, Gierthmuehlen M. Effect of cardiac-cycle-synchronized selective vagal stimulation on heart rate and blood pressure in rats. *Adv Ther*. 2016;33:1246–1261. https://doi.org/10.1007/s12325-016-0348-z.
13. GBD 2013 Mortality and Causes of Death Collaborators. Global, regional, and national age-sex specific all-cause and cause-specific mortality for 240 causes of death, 1990–2013: a systematic analysis for the Global Burden of Disease Study 2013. *Lancet*. 2015;385:117–171. https://doi.org/10.1016/S0140-6736(14)61682-2.
14. Capilupi MJ, Kerath SM, Becker LB. Vagus nerve stimulation and the cardiovascular system. *Cold Spring Harb Perspect Med*. 2020;10:a034173. https://doi.org/10.1101/cshperspect.a034173.
15. Binkley PF, Haas GJ, Starling RC, et al. Sustained augmentation of parasympathetic tone with angiotensin-converting enzyme inhibition in patients with congestive heart failure. *J Am Coll Cardiol*. 1993;21:655–661. https://doi.org/10.1016/0735-1097(93)90098-L.
16. Gold MR, Van Veldhuisen DJ, Hauptman PJ, et al. Vagus nerve stimulation for the treatment of heart failure: The INOVATE-HF Trial. *J Am Coll Cardiol*. 2016;68:149–158. https://doi.org/10.1016/j.jacc.2016.03.525.
17. Premchand RK, Sharma K, Mittal S, et al. Autonomic regulation therapy via left or right cervical vagus nerve stimulation in patients with chronic heart failure: results of the ANTHEM-HF trial. *J Card Fail*. 2014;20:808–816. https://doi.org/10.1016/j.cardfail.2014.08.009.
18. De Ferrari GM, Crijns HJGM, Borggrefe M, et al. Chronic vagus nerve stimulation: a new and promising therapeutic approach for chronic heart failure. *Eur Heart J*. 2011;32:847–855. https://doi.org/10.1093/eurheartj/ehq391.
19. Ardell JL, Randall WC. Selective vagal innervation of sinoatrial and atrioventricular nodes in canine heart. *Am J Physiol*. 1986;251:H764–H773. https://doi.org/10.1152/ajpheart.1986.251.4.H764.
20. De Ferrari GM, Stolen C, Tuinenburg AE, et al. Long-term vagal stimulation for heart failure: eighteen month results from the NEural Cardiac TherApy foR Heart Failure (NECTAR-HF) trial. *Int J Cardiol*. 2017;244:229–234. https://doi.org/10.1016/j.ijcard.2017.06.036.
21. Anand IS, Konstam MA, Klein HU, et al. Comparison of symptomatic and functional responses to vagus nerve stimulation in ANTHEM-HF, INOVATE-HF, and NECTAR-HF. *ESC Heart Fail*. 2020;7:75–83. https://doi.org/10.1002/ehf2.12592.
22. Sharma K, Premchand RK, Mittal S, et al. Long-term follow-up of patients with heart failure and reduced ejection fraction receiving autonomic regulation therapy in the ANTHEM-HF pilot study. *Int J Cardiol*. 2021;323:175–178. https://doi.org/10.1016/j.ijcard.2020.09.072.
23. Thompson N, Ravagli E, Mastitskaya S, et al. Organotopic organization of the cervical vagus nerve. Preprint. Posted online January 26, 2023. https://doi.org/10.1101/2022.02.24.481810
24. Nicolai EN, Settell ML, Knudsen BE, et al. Sources of off-target effects of vagus nerve stimulation using the helical clinical lead in domestic pigs. *J Neural Eng*. 2020;17:046017. https://doi.org/10.1088/1741-2552/ab9db8.
25. Strauss I, Valle G, Artoni F, et al. Characterization of multi-channel intraneural stimulation in transradial amputees. *Sci Rep*. 2019;9:19258. https://doi.org/10.1038/s41598-019-55591-z.
26. Pelot NA, Goldhagen GB, Cariello JE, et al. Quantified morphology of the cervical and subdiaphragmatic vagus nerves of human, pig, and rat. *Front Neurosci*. 2020;14:601479. https://doi.org/10.3389/fnins.2020.601479.
27. Boretius T, Badia J, Pascual-Font A, et al. A transverse intrafascicular multichannel electrode (TIME) to interface with the peripheral nerve. *Biosens Bioelectron*. 2010;26:62–69. https://doi.org/10.1016/j.bios.2010.05.010.
28. Cutrone A, Del Valle J, Santos D, et al. A three-dimensional self-opening intraneural peripheral interface (SELINE). *J Neural Eng*. 2015;12:016016. https://doi.org/10.1088/1741-2560/12/1/016016.
29. Strauss I, Zinno C, Giannotti A, Ottaviani MM, Recchia FA, Micera S. Adaptation and optimization of an intraneural electrode to interface with the cervical vagus nerve. Paper presented at: 10th International IEEE/EMBS Conference on Neural Engineering (NER); May 4–6, 2021; Italy.
30. Ferraro D, D'Alesio G, Camboni D, et al. Implantable fiber Bragg grating sensor for continuous heart activity monitoring: ex-vivo and in-vivo validation. *IEEE Sensors J*. 2021;21:14051–14059. https://doi.org/10.1109/JSEN.2021.3056530.
31. Lionetti V, Romano SL, Bianchi G, et al. Impact of acute changes of left ventricular contractility on the transvalvular impedance: validation study by pressure-volume loop analysis in healthy pigs. *PLoS One*. 2013;8:e80591. https://doi.org/10.1371/journal.pone.0080591.
32. Wu Y, Jiang D, Demosthenous A. A multi-channel stimulator with high-resolution time-to-current conversion for vagal-cardiac neuromodulation. *IEEE Trans Biomed Circuits Syst*. 2021;15:1186–1195. https://doi.org/10.1109/TBCAS.2021.3139996.
33. Haberbusch M, Frullini S, Moscato F. A numerical model of the acute cardiac effects provoked by cervical vagus nerve stimulation. *IEEE Trans Biomed Eng*. 2022;69:613–623. Published correction appears in *IEEE Trans Biomed Eng*. 2022;69:3275. https://doi.org/10.1109/TBME.2021.3102416
34. Parati G, Saul JP, Di Rienzo M, Mancia G. Spectral analysis of blood pressure and heart rate variability in evaluating cardiovascular regulation. A critical appraisal. *Hypertension*. 1995;25:1276–1286. https://doi.org/10.1161/01.HYP.25.6.1276.
35. Buschman HP, Storm CJ, Duncker DJ, Verdouw PD, van der Aa HE, van der Kemp P. Heart rate control via vagus nerve stimulation. *Neuromodulation*. 2006;9:214–220. https://doi.org/10.1111/j.1525-1403.2006.00062.x.
36. Plachta DTT, Gierthmuehlen M, Cota O, et al. Blood pressure control with selective vagal nerve stimulation and minimal side effects. *J Neural Eng*. 2014;11:036011. https://doi.org/10.1088/1741-2560/11/3/036011.
37. Blanz SL, Musselman ED, Settell ML, et al. Spatially selective stimulation of the pig vagus nerve to modulate target effect versus side effect. *J Neural Eng*. 2023;(1):20. https://doi.org/10.1088/1741-2552/acb3fd.
38. Frink Jr EJ, Malan TP, Atlas M, Dominguez LM, DiNardo JA, Brown BR Jr. Clinical comparison of sevoflurane and isoflurane in healthy patients. *Anesth Analg*. 1992;74:241–245.
39. Graf BM, Vicenzi MN, Bosnjak ZJ, Stowe DF. The comparative effects of equimolar sevoflurane and isoflurane in isolated hearts. *Anesth Analg*. 1995;81:1026–1032.
40. Malan Jr TP, DiNardo JA, Isner RJ, et al. Cardiovascular effects of sevoflurane compared with those of isoflurane in volunteers. *Anesthesiology*. 1995;83:918–928. https://doi.org/10.1097/00000542-199511000-00004.
41. Loushin MK. The effects of anesthetic agents on cardiac function. In: Iaizzo PA, ed. *Handbook of Cardiac Anatomy, Physiology, and Devices*. Humana Press Inc; 2005:171–180.